Electronic Supplementary Material (ESI) for Nanoscale.

Supplementary Information:

Synthesis and characterisation of thin-film platinum disulfide and platinum sulfide

Conor P. Cullen[1,2], Cormac Ó Coileáin [1,2], John B. McManus[1,2], Oliver Hartwig[3], David McCloskey[4], Georg S. Duesberg[1,2,3], Niall McEvoy[1,2]

[1] School of Chemistry, Trinity College Dublin, Dublin 2, D02 PN40, Ireland

[2] AMBER Centre, CRANN Institute, Trinity College Dublin, Dublin 2, Ireland

[3] Institute of Physics, EIT 2, Faculty of Electrical Engineering and Information Technology, Universität der Bundeswehr München, 85579 Neubiberg, Germany

[4] School of Physics, Trinity College Dublin, Dublin 2, Ireland

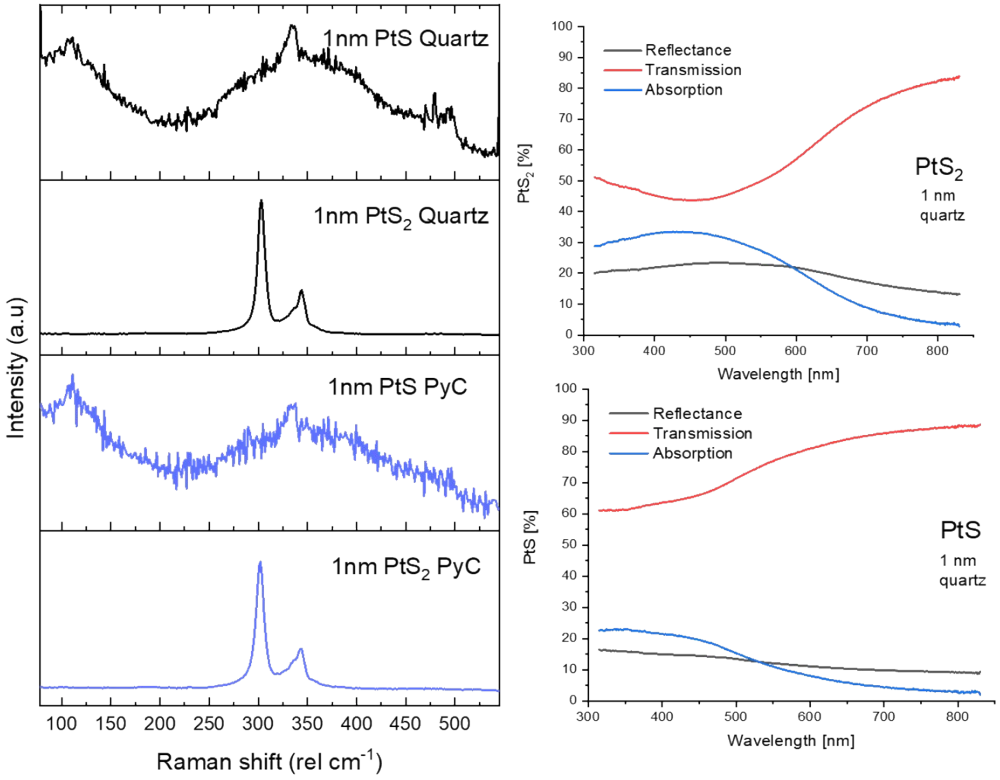

Figure S1. (a) Raman spectra of 1 nm PtS_2 and PtS films synthesized on quartz and PyC substrates acquired with 532 nm excitation. **(b)** Optical spectra measured for platinum sulfide films synthesized on quartz.

Fig.S1(a) shows Raman spectra which indicate the successful synthesis of PtS and PtS_2 on quartz and pyrolytic carbon (PyC) substrates.

1 nm PtS_2 and PtS films were deposited on quartz substrates to investigate their optical properties. Fig.S1(b) shows reflectance, transmission and absorption spectra for both films between 314-830 nm. The PtS_2 film shows relatively uniform reflectivity across the range at ~20%. An absorption maximum is seen of 34% at ~440 nm while being >70% transparent for wavelengths greater than ~680 nm. The PtS film has lower, but also roughly uniform, reflectivity of ~15%. PtS also shows consistently lower absorption across the range with a maximum of 23% at ~350 nm and >70% transmission for wavelengths >490 nm. The measurements were taken using a UV-vis spectrophotometer with an integrating sphere attachment (Perkin Elmer LAMBDA 650). A lens system was used to collect the spectrum of a 1 mm diameter area. The total diffuse transmission and specular and diffuse reflection were measured. The difference between these two measurements was used to calculate the absorption of the films.

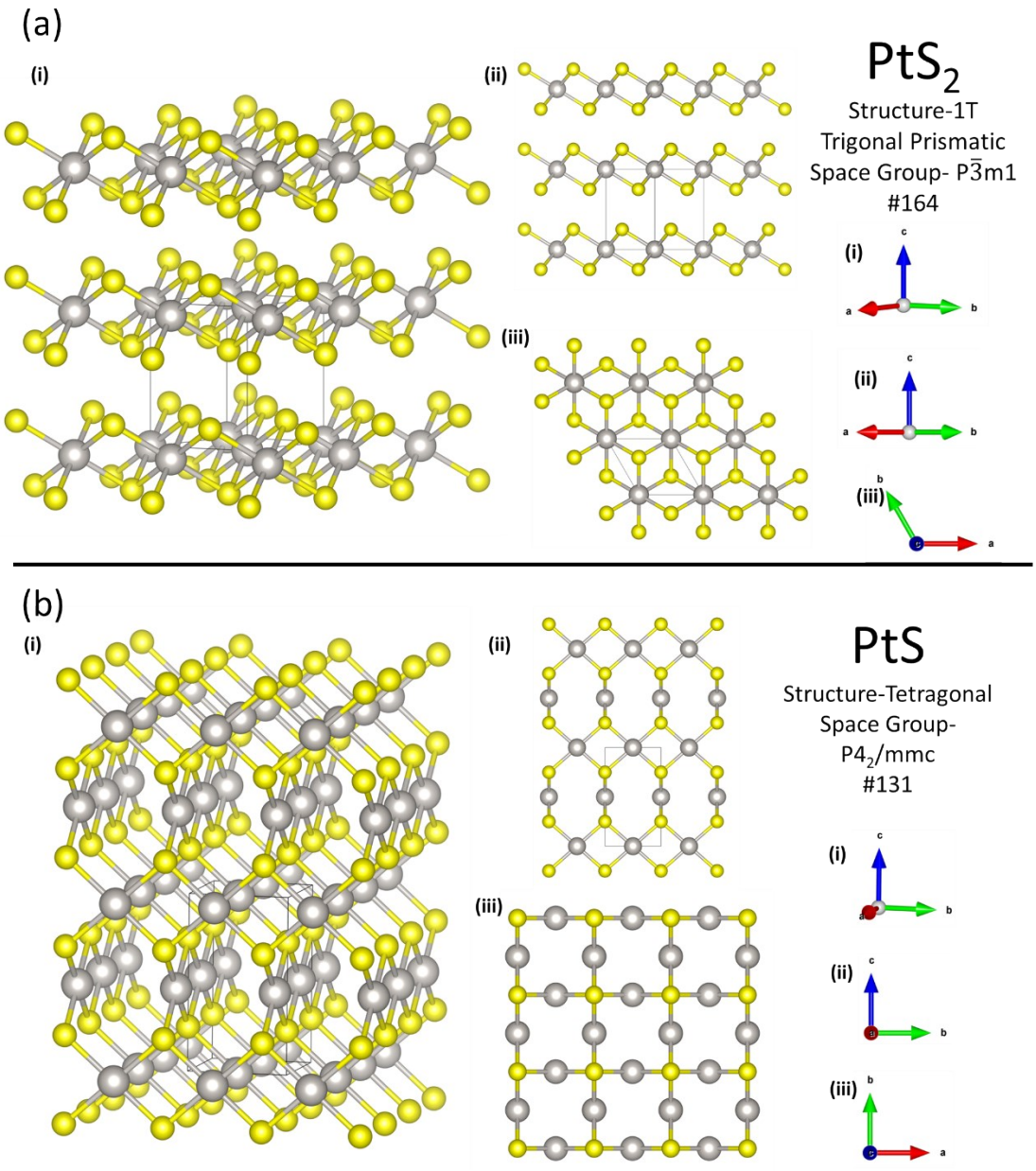

Figure S2. Diagrams of the atomic structure for **(a)** PtS_2 and **(b)** PtS

Structural representations

Atomic structural representations for each material were generated using VESTA 3 software.[1]

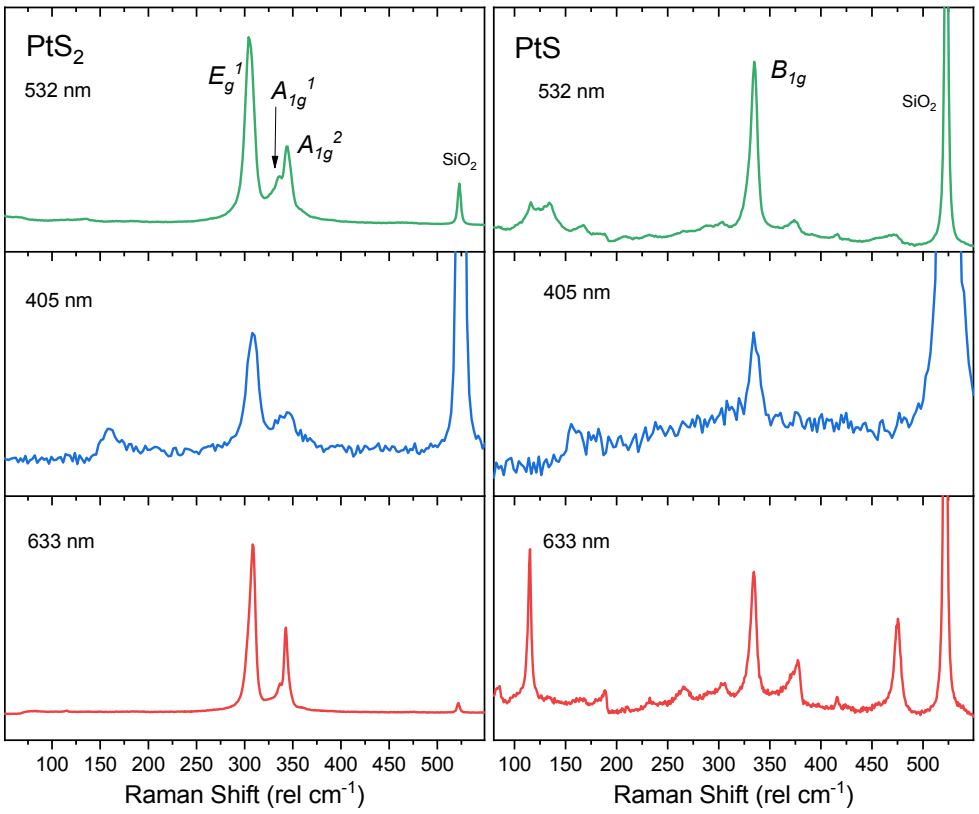

Figure S3. (a) Raman spectra of a 5 nm PtS_2 film using different wavelength Raman lasers. **(b)** Raman spectra of a 5 nm PtS film using different wavelength Raman lasers

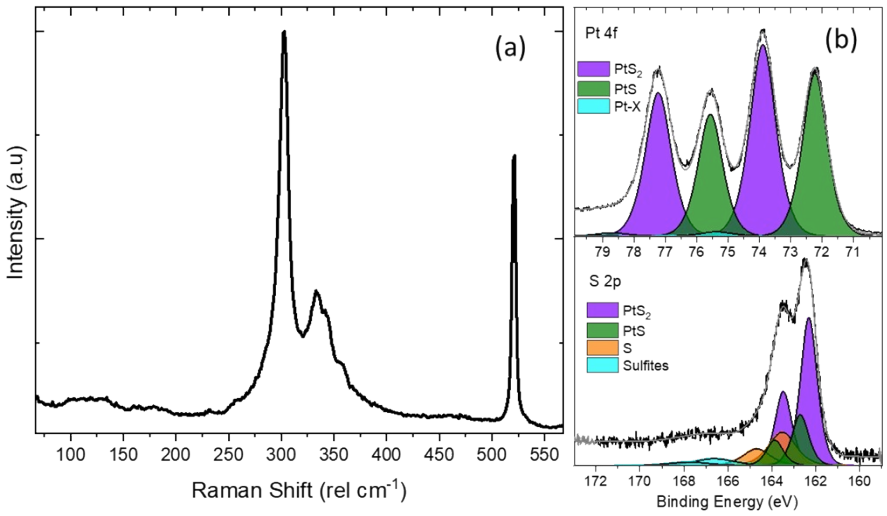

Figure S4. (a) Raman spectra of a mixed PtS_2-PtS film grown at 400 °C. **(b)** XPS Pt 4f and S 2p core-level spectra of the mixed film showing the relevant components of each material

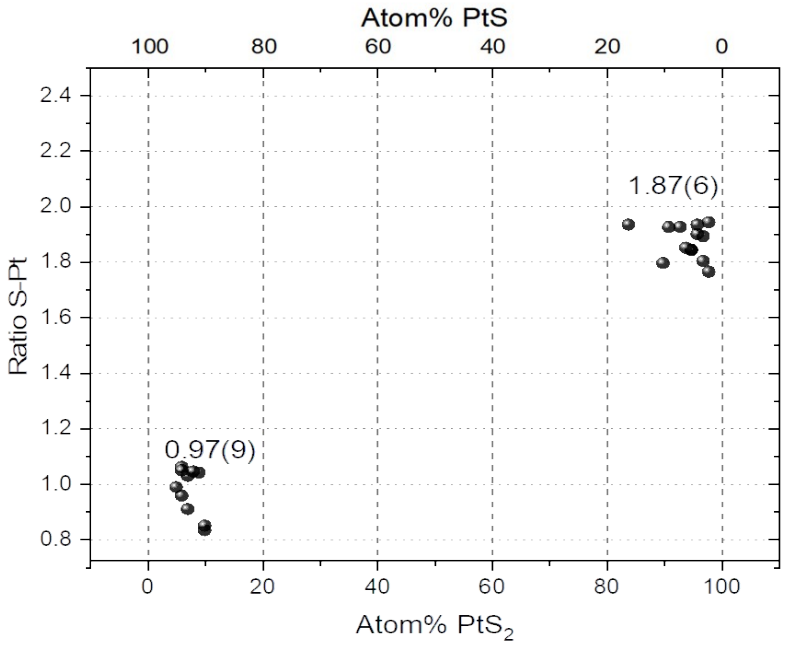

Figure S5. Plot of the S-Pt ratio for 24 Pt sulfide films as calculated by comparison of relative XPS peak areas showing the clusters for PtS and PtS_2.

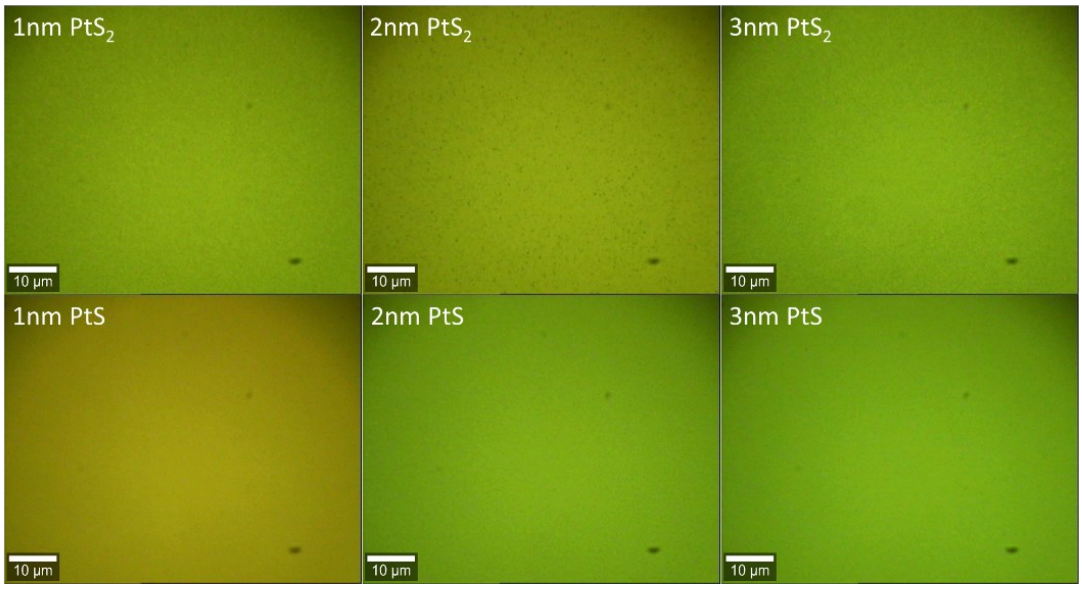

Figure S6. Optical images with a 100x microscope objective of the surface of 1, 2, and 3 nm PtS_2 and PtS films.

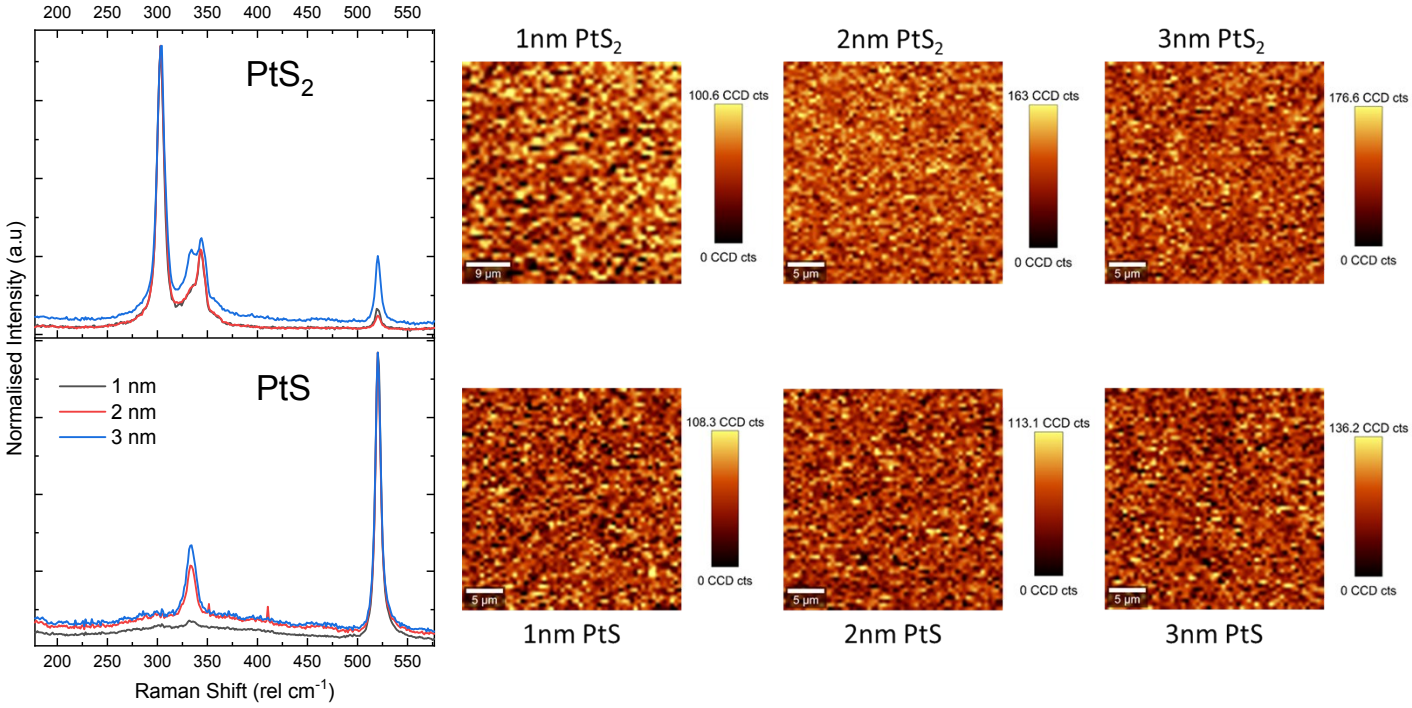

Figure S7. Averaged Raman spectra for 1, 2, and 3 nm PtS_2 and PtS films. Raman intensity maps of the surface of the films show consistent signal across the surface for all films.

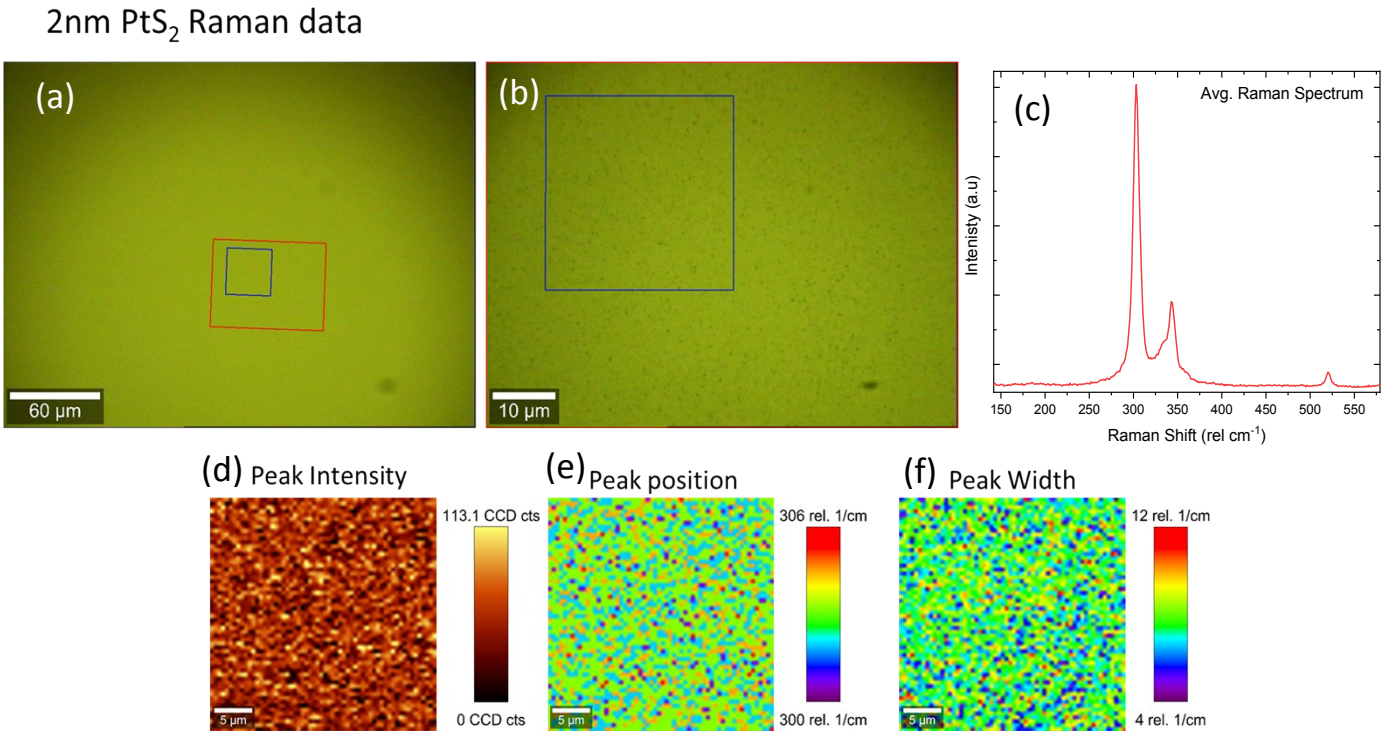

Figure S8. (a) Optical image with a 20x microscope objective of the surface of a 2 nm PtS_2 film, with a red box showing the area in **(b)** and a blue box showing the area mapped by Raman spectroscopy. **(b)** A 100x microscope objective image, with the blue box representing the area mapped by Raman spectroscopy. **(c)** Average Raman spectra of the film. **(d)** E_g^1 Raman peak intensity map. **(e)** Raman peak position map. **(f)** Raman peak width (FWHM) map.

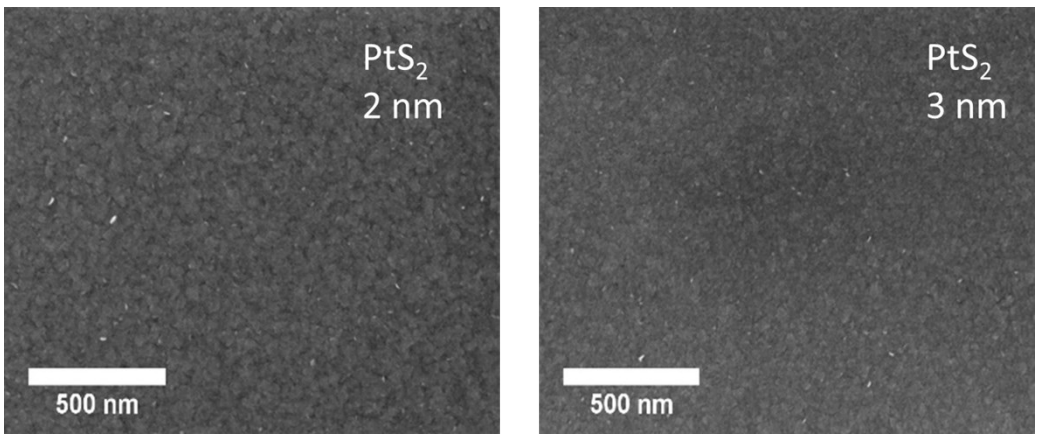

Figure S9. SEM images of PtS_2 films synthesized

from 2 and 3 nm Pt films.

AFM analysis of Pt, PtS and PtS_2 films

Atomic force microscopy (AFM) was performed on a Bruker Multimode 8 with ScanAsyst Air AFM probes in ScanAsyst Air 146 mode. The applied scan rate was 1 Hz with an image resolution of 512x512 points. Peak-force tapping mode was used to obtain the topography. The acquired data was processed using Gwyddion software.[2]

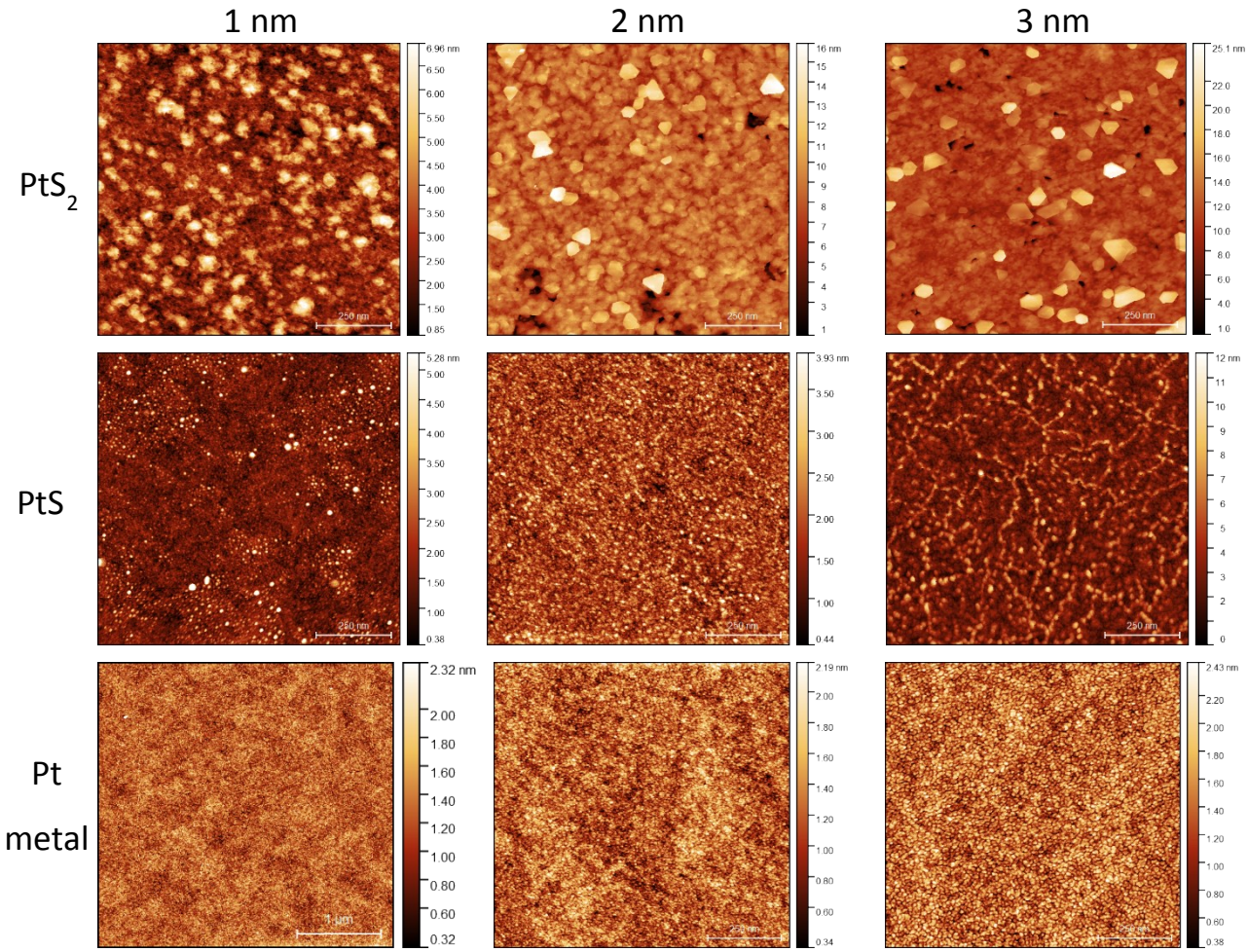

Figure S10. AFM maps of the surface of 1, 2, and 3 nm PtS_2, PtS, and as-deposited Pt metal films. Scale bar 250 nm, except for 1 nm Pt metal (1 µm).

Determining the theoretical film thickness after conversion of a Pt film to PtS_2 or PtS is difficult due to the random orientation of the crystallites and the layered/non-layered nature of the materials. To

roughly estimate the film expansion, we use the unit cell volume for the respective materials, determined using literature values for PtS_2,[3] PtS,[4] and Pt metal.[5] This yields an estimate for film volume expansion of 3.5x for PtS_2 and 4.7x for a PtS film. This greater thickness for PtS films over PtS_2 is also seen in our measured film thicknesses. $PtSe_2$ synthesised through a similar synthesis process was found to have an expansion of ~4x from the as-deposited platinum.[6]

Table S1. AFM measured film properties.

Film	1nm Pt metal	1nm PtS_2	1nm PtS	2nm Pt metal	2nm PtS_2	2nm PtS	3nm Pt metal	3nm PtS_2	3nm PtS
Roughness (nm)	0.297	1.04	0.63	0.3	1.57	0.52	0.35	2.45	1.33
Expansion factor	-	1.4	3.1	-	3.2	5.9	-	2.5	-
Thickness (nm)	1.13	1.57	3.53	2.43	7.77	14.37	3.74	9.37	-

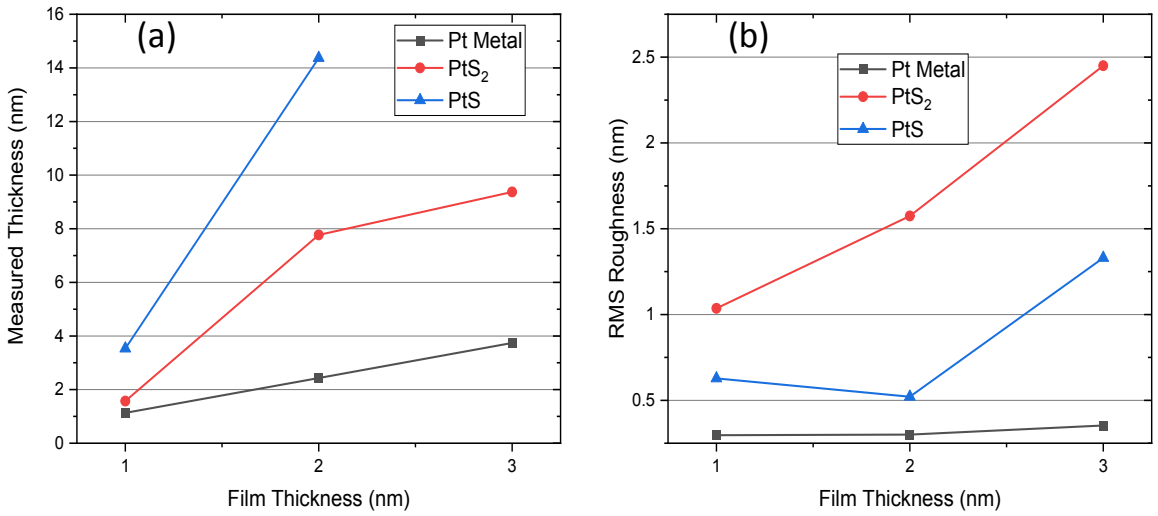

Figure S11. (a) Graph of measured film thickness and **(b)** surface RMS roughness against intended initial Pt metal thickness for the AFM images in Fig.S10.

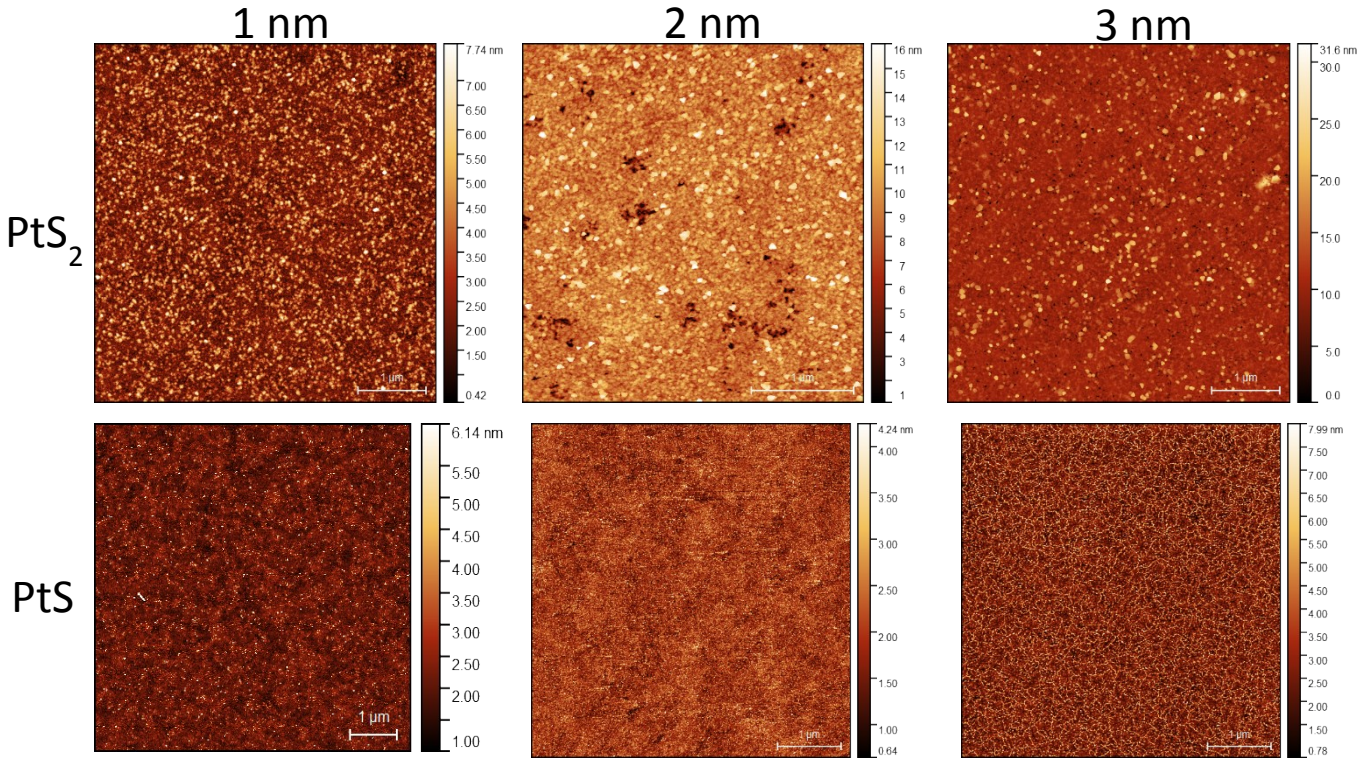

Figure S12. AFM maps of larger areas of the surface of 1, 2, and 3 nm PtS_2 and PtS films. Scale bar 1 µm.

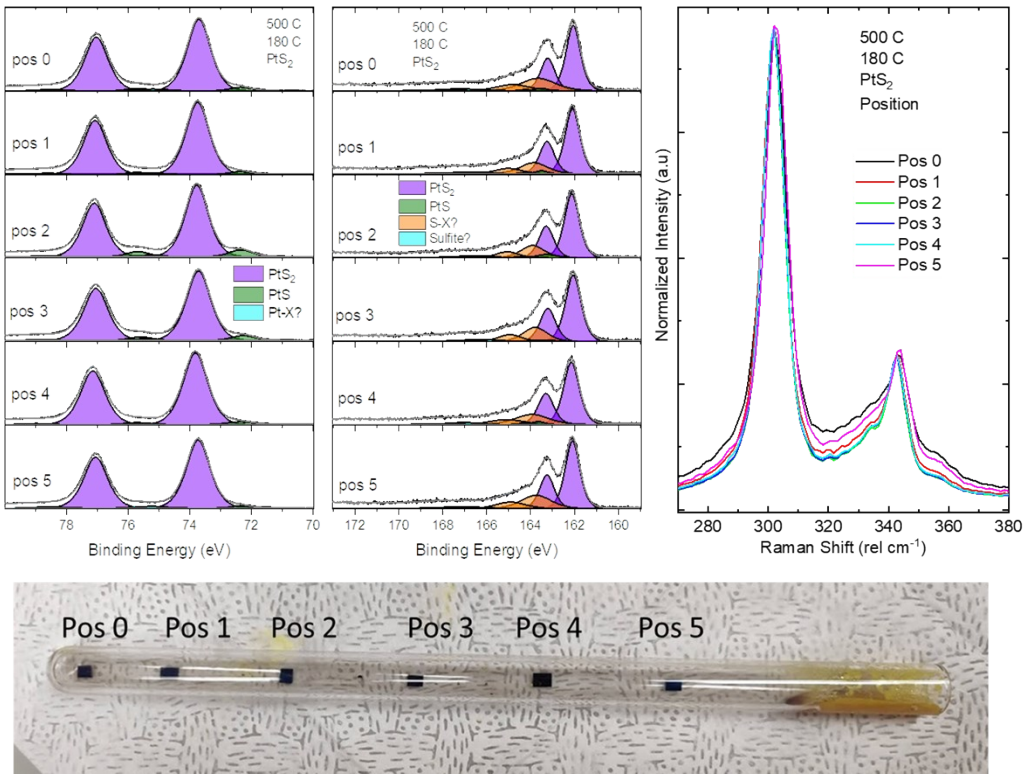

Figure S13. (a) XPS spectra of 1 nm PtS_2 films synthesized along the length of the internal quartz tube. **(b)** Raman spectra of the PtS_2 films. **(c)** Picture of the quartz tube showing the positions of the substrates.

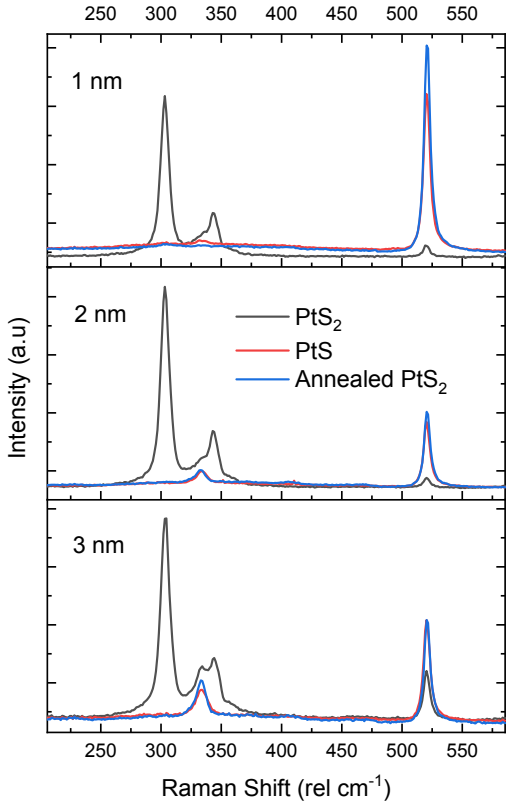

Figure S14. Raman spectra for 1, 2, and 3 nm films of PtS_2, PtS, and PtS_2 films after 600 °C annealing in an inert environment at ~1 mbar for 30 minutes, showing a change from PtS_2 to PtS Raman signal.

References

S1. K. Momma and F. Izumi, *J. Appl. Crystallogr.*, 2011, **44**, 1272-1276.

S2. D. Nečas and P. Klapetek, *Cent. Eur. J. Phys.*, 2012, **10**, 181-188.

S3. H. A. H. Mohammed, G. M. Dongho-Nguimdo and D. P. Joubert, *Materials Today Communications*, 2019, DOI: 10.1016/j.mtcomm.2019.100661, 100661.

S4. V. I. Rozhdestvina, A. V. Ivanov, M. A. Zaremba, O. N. Antsutkin and W. Forsling, *Crystallogr. Rep.*, 2008, **53**, 391-397.

S5. W. P. Davey, *Phys. Rev.*, 1925, **25**, 753-761.

S6. C. Yim, V. Passi, M. C. Lemme, G. S. Duesberg, C. Ó Coileáin, E. Pallecchi, D. Fadil and N. McEvoy, *npj 2D Materials and Applications*, 2018, **2**, 5.